Review of Thermal Joint Resistance Models for Nonconforming Rough Surfaces

M. Bahrami
Post-doctoral Fellow
Mem. ASME

J. R. Culham
Associate Professor, Director
Mem. ASME

M. M. Yananovich
Distinguished Professor Emeritus
Fellow ASME

G. E. Schneider
Professor

Microelectronics Heat Transfer Laboratory,
Department of Mechanical Engineering,
University of Waterloo,
Waterloo, ON N2L 3G1, Canada

The thermal contact resistance (TCR) in a vacuum is studied. The TCR problem is divided into three different parts: geometrical, mechanical, and thermal. Each problem includes a macro- and microscale subproblem; existing theories and models for each part are reviewed. Empirical correlations for microhardness, and the equivalent (sum) rough surface approximation, are discussed. Suggested correlations for estimating the mean absolute surface slope are summarized and compared with experimental data. The most common assumptions of existing thermal analyses are summarized. As basic elements of thermal analyses, spreading resistance of a circular heat source on a half-space and flux tube are reviewed; also existing flux tube correlations are compared. More than 400 TCR data points collected by different researchers during the last 40 *years are grouped into two limiting cases: conforming rough and elastoconstriction. Existing TCR models are reviewed and compared with the experimental data at these two limits. It is shown that the existing theoretical models do not cover both of the above-mentioned limiting cases. This review article cites 58 references.* [DOI: 10.1115/1.2110231]

Introduction

Heat transfer through interfaces formed by the mechanical contact of two nonconforming rough solids occurs in a wide range of applications: microelectronics cooling, spacecraft structures, satellite bolted joints, nuclear engineering, ball bearings, and heat exchangers. Analytical, experimental, and numerical models have been developed to predict thermal contact resistance since the 1930s. Several hundred papers on thermal contact resistance have been published which illustrates the importance of this topic, and also indicates that the development of a general predictive model is difficult. Real interaction between two surfaces occurs only over microscopic contacts. The real area of contact, the total area of all microcontacts, is typically a small fraction of the nominal contact area [1,2]. As illustrated in Fig. 1, the macroscopic contact region arises due to surface curvature or out-of-flatness of bodies; the microcontacts form at the interface between contacting asperities of rough surfaces. In these situations heat flow experiences two stages of resistance in series, macroscopic and microscopic constriction resistance [3,4]. This phenomenon leads to a relatively high temperature drop across the interface.

Thermal energy can be transferred between contacting bodies by three different modes, (i) conduction at the microcontacts, (ii) conduction through the interstitial fluid in the gap between the contacting solids, and (iii) thermal radiation across the gap. The radiation heat transfer remains small and can be neglected for surface temperatures up to 700 K [5,6]. In this study the interstitial fluid is assumed to be absent (vacuum), thus the only remaining heat transfer mode is conduction at the microcontacts. The TCR in the presence of an interstitial gas is studied in Refs. [7,8].

Thermal contact resistance (TCR) problems consist of three different problems: geometrical, mechanical, and thermal. Figure 2 illustrates the thermal contact resistance analysis and its components. The heart of a TCR analysis is the mechanical part. Any solution for the mechanical problem requires that the geometry of the contacting surfaces (macro and micro) be quantitatively described. The mechanical problem also includes two parts: macro- or large-scale contact and micro- or small-scale contact. The mechanical analysis determines the macrocontact radius, a_L, and the pressure distribution for the large-scale problem. For the microcontact problem, separation between the mean contacting planes, microcontact size, density of microcontacts, and the relative microcontact radius are calculated. The macro- and the micromechanical problems are coupled. The thermal analysis, based on the results of the mechanical analysis, is then used to calculate the microscopic and macroscopic thermal resistances.

The geometrical and mechanical analyses of the TCR can be affected as a result of heat transfer and temperature changes in the vicinity of the contact area. For instance, thermal stresses and thermal expansions can lead to changes in surface characteristics and the stress field which in turn can affect the geometrical and mechanical analyses, respectively. However, in this study, these influences are assumed to have secondary order effects and are thus neglected. As a result of this simplification, the three components of the thermal contact resistance problem can be decoupled as shown in Fig. 2.

Geometrical Analysis

It is necessary to consider the effect of both surface roughness and surface curvature/out-of-flatness on the contact of nonconforming rough surfaces. Therefore, the geometrical analysis is divided into micro and macro parts.

Microgeometrical Analysis. All solid surfaces are rough, and this roughness or surface texture can be thought of as the surface deviation from the nominal topography. Surface textures can be created using many different processes. Most artificial engineered surfaces, such as those produced by grinding or machining, have a pronounced "lay." Generally, the term "Gaussian surface" is used to refer to a surface with isotropic asperities, randomly distributed over the surface. It is not easy to produce a wholly isotropic roughness. The usual procedure for experimental purposes is to air-blast a metal surface with a cloud of fine particles, in the manner of shot peening, which gives rise to a random rough surface. According to Liu et al. [9] five types of instruments are currently available for measuring the surface topography: stylus-type surface profilometer, optical (white-light interference) measurements, scanning electron microscope (SEM), atomic force microscope (AFM), and scanning tunneling microscope (STM). Among these, the first two instruments are usually used for macro-to-macro asperity measurements, whereas the others may

Transmitted by Assoc. Editor J. G. Simmonds.

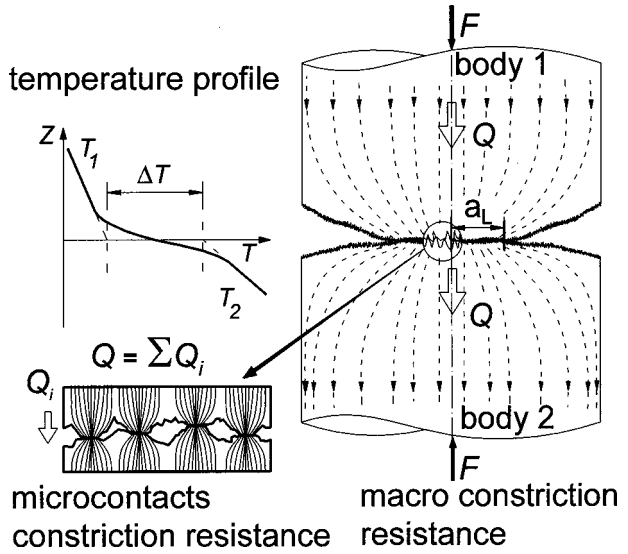

Fig. 1 Macro- and microthermal constriction/spreading resistances

be used for micro- or nanometric measurements. Surface texture is most commonly measured by a profilometer, which draws a stylus over a sample length of the surface. A datum or centerline is established by finding the straight line, or circular arc in the case of round components, from which the mean square deviation is a minimum. The arithmetic average of the absolute values of the measured profile height deviations is R_a, taken within a sampling length from the graphical centerline [10]. The value of R_a is

$$R_a = \frac{1}{L}\int_0^L |z(x)|dx \tag{1}$$

where L is the sampling length in the x direction and z is the measured value of the surface height along this length. When the surface is Gaussian, the standard deviation σ is identical to the rms value, R_q:

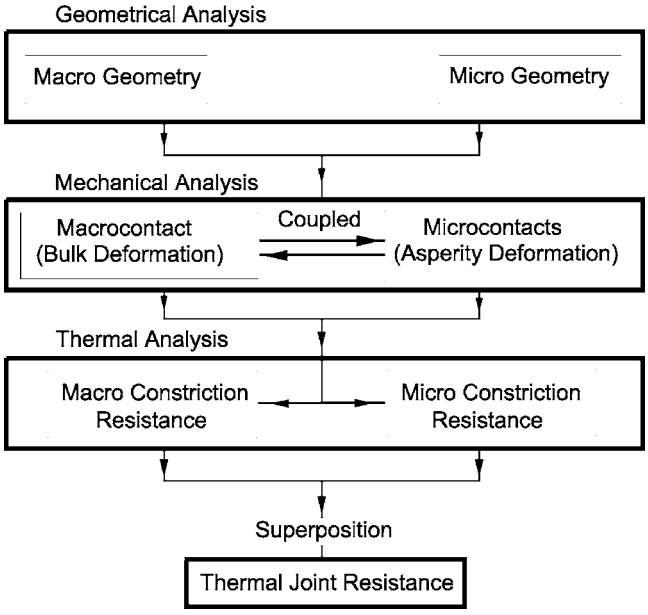

Fig. 2 Thermal contact resistance modeling flow diagram

Table 1 Correlations for *m*, Gaussian surfaces

Reference	Correlation
Tanner and Fahoum [12]	$m=0.152\ \sigma^{0.4}$
Antonetti et al. [13]	$m=0.124\ \sigma^{0.743}$, $\sigma \leqslant 1.6\ \mu$m
Lambert and Fletcher [14]	$m=0.076\ \sigma^{0.52}$

$$\sigma = R_q = \sqrt{\frac{1}{L}\int_0^L z^2(x)dx} \tag{2}$$

For a Gaussian surface, Ling [11] showed that the average and rms heights are related as follows:

$$R_q \approx \sqrt{\frac{\pi}{2}}R_a \approx 1.25R_a \tag{3}$$

Similarly, the absolute average and rms asperity slopes, m and m', respectively, can be determined across the sampling length from the following:

$$m = \frac{1}{L}\int_0^L \left|\frac{dz(x)}{dx}\right| dx, \quad m' = \sqrt{\frac{1}{L}\int_0^L \left(\frac{dz(x)}{dx}\right)^2 dx} \tag{4}$$

Mikic and Rohsenow [4] showed that for Gaussian surfaces the relationship between the average and rms values of the asperity slopes is $m' \approx 1.25m$. Tanner and Fahoum [12] and Antonetti et al. [13], using published experimental surface data, suggested empirical correlations to relate rms asperity slope, m', to average roughness, R_a. Lambert and Fletcher [14], also using the same method, correlated the absolute average asperity slopes, m, as a function of rms roughness in micrometers; correlations for m are summarized in Table 1. Figure 3 shows the comparison between these correlations and experimental data. As shown in Fig. 3, the uncertainty of the above correlations is high, and use of these correlations is justifiable only where the surface slope is not reported and/or a rough estimation of m is needed.

Equivalent (Sum) Rough Surface. According to the examination of the microgeometry with equivalent magnitude in the vertical direction and in the traversing direction, asperities seem to have curved shapes at their tops [15]. A common way to model the surface roughness is to represent the surface asperities by simple geometrical shapes with a probability distribution for the different asperity parameters involved. One of the first presentations to use this asperity-based model is found in Coulomb's work

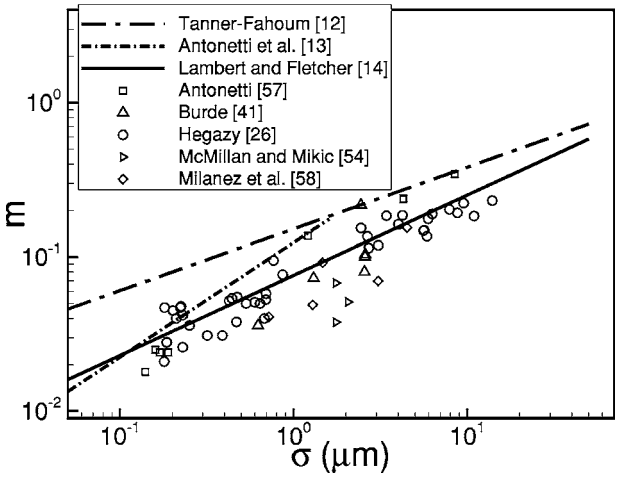

Fig. 3 Comparison between correlations for *m* and experimental data

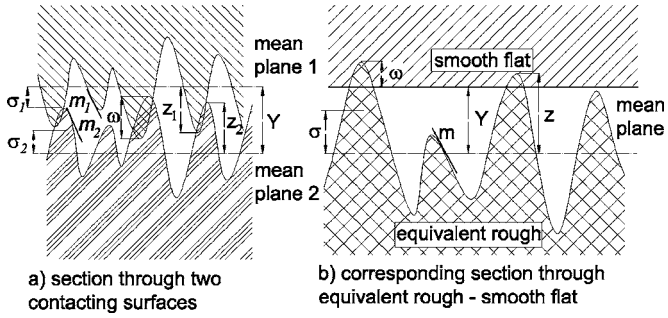

Fig. 4 Equivalent contact of conforming rough surfaces

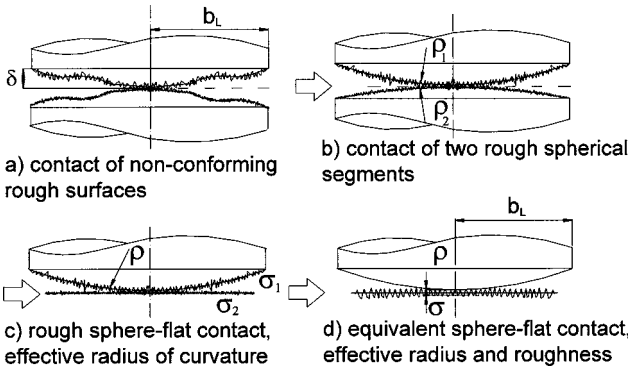

Fig. 5 Flow diagram of geometrical modeling

in 1782. To explain the laws of friction, he assumed that the asperities possessed a spherical shape, all of which had the same radius and the same summit altitude. Greenwood and Williamson [1] assumed that each asperity summit had a spherical shape whose height above a reference plane had a normal (Gaussian) probability density function. Williamson et al. [16] have shown experimentally that many of the techniques used to produce engineering surfaces give a Gaussian distribution of surface heights.

The solution of any contact mechanics problem requires that the geometry of the intersection and overlap of the two undeformed surfaces be known as a function of their relative position. A genuine treatment of two rough surfaces is complicated by the difficulty of describing the unit event, the formation of a single contact spot. For example, if both surfaces are covered by spheres, it is necessary to study the contact of one sphere on the shoulder of another, and then evaluate the probabilities of different degrees of misalignment, in order to get the average unit event. A nongenuine treatment is comparatively simple: both surfaces are taken to be rough with normal distributions. The statistical treatment now concerns the probability of the sum of two heights (which is also normally distributed) exceeding the separation, and this is exactly equivalent to a distribution of a single variable [17]. Following the nongenuine approach, the contact between Gaussian rough surfaces can be considered as the contact between a single Gaussian surface, having the effective (sum) surface characteristics, placed in contact with a perfectly smooth flat surface. Also, since the slope, m, of a profile is proportional to the difference between adjacent equispaced ordinates, m is Gaussian if the profile is Gaussian [18]. This simplification was used by many researchers such as Clausing and Chao [3], Cooper et al. [19], Francis [20], and Johnson [21]. The equivalent roughness and surface slope can be calculated from

$$\sigma = \sqrt{\sigma_1^2 + \sigma_2^2} \quad \text{and} \quad m = \sqrt{m_1^2 + m_2^2} \tag{5}$$

A contact model based on the sum (equivalent) surface circumvents the problem of misalignment of contacting peaks; in addition, the sum surface sees peak to valley and peak to saddle contacts. The sum surface of two Gaussian surfaces is itself Gaussian and if parent surfaces are not exactly Gaussian, the sum (equivalent) surface will be closer to Gaussian than the parent surfaces. Additionally, the sum surface will be in general less anisotropic than the two contacting surfaces, thus the Gaussian sum surface is a reasonable basis for a general contact model [20]. Figure 4 shows a normal section through the contact, in which the surfaces are imagined to overlap without deforming, and the equivalent rough or sum surface of the contact in the same normal section. The overlap geometry as a function of the mean separation, Y, of the undeformed surfaces is thus given directly and exactly by the shape of the equivalent rough surface. The number of microcontacts formed is simply the number of equivalent surface peaks that have $Z \geqslant Y$.

Macrogeometrical Analysis. Many studies on thermal contact resistance assume an ideal uniform distribution of microcontacts, i.e., conforming rough surface models. Such approaches are successful where the macroscopic nonuniformity of the contact is negligible. However, no real engineering surfaces are perfectly flat, thus the influence of macroscopic nonuniformity can never be ignored. Considering the waviness or out-of-flatness of contacting surfaces in a comprehensive manner is very complex because of the case-by-case nature of the waviness. Certain simplifications must be introduced to describe the macroscopic topography of surfaces by a few parameters. A sphere is the simplest example of a macroscopically homogeneous surface. Specifically, its profile is described only by its radius. Theoretical approaches by Clausing and Chao [3], Mikic and Rohsenow [4], Yovanovich [22], Nishino et al. [23], and Lambert and Fletcher [14] assume that a spherical profile may approximate the shape of the macroscopic nonuniformity. According to Lambert [24] this assumption is justifiable because nominally flat engineering surfaces are often spherical or crowned (convex) with a monotonic curvature in at least one direction.

In static frictionless contact of solids, the contact stresses depend only upon the relative profile of the two surfaces, i.e., upon the shape of the interstitial gap between them before loading. The actual system geometry may be replaced, without loss of generality, by a flat surface and a profile, which results in the same undeformed gap between the surfaces [21]. For convenience, all elastic deformations can be considered to occur in one body, which has an effective elastic modulus, and the other body is assumed to be rigid. The effective elastic modulus can be found from

$$\frac{1}{E'} = \frac{1-\nu_1^2}{E_1} + \frac{1-\nu_2^2}{E_2} \tag{6}$$

where E and ν are the Young's modulus and Poisson's ratio, respectively. For the contact of two spheres, the effective radius of curvature is

$$\frac{1}{\rho} = \frac{1}{\rho_1} + \frac{1}{\rho_2} \tag{7}$$

For relatively large radii of curvature, where the contacting surfaces are nearly flat, an approximate geometrical relationship can be found between radius of curvature and the maximum out-of-flatness [3],

$$\rho = \frac{b_L^2}{2\delta} \tag{8}$$

where δ is the maximum out-of-flatness of the surface.

Figure 5 details the procedure, which has been used widely for the geometric modeling of the actual contact between two curved rough bodies. As a result of the above, the complex geometry of

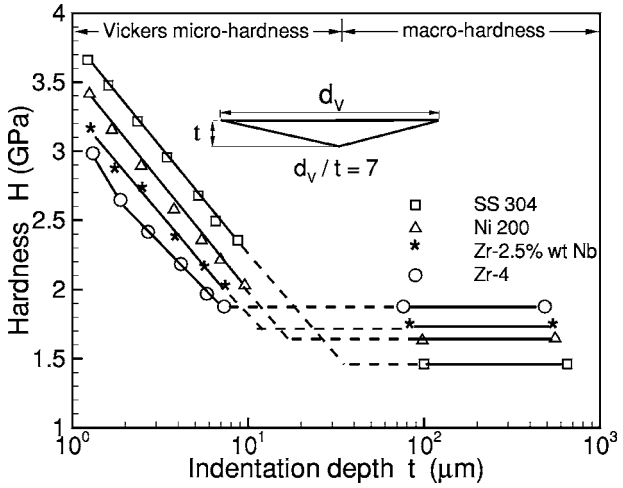

Fig. 6 Measured hardness and microhardness [26]

nonconforming rough contacts can be simplified to the contact of the equivalent truncated spherical surface with the equivalent rough flat.

Microhardness. Hardness is defined as the resistance to permanent deformation; hardness definitions and tests can be found in various standard textbooks, e.g., those by Tabor [2] and Mott [25]. The most common hardness testing method is the static indentation. In a static indentation test, a steady load is applied to an indenter which may be a ball, cone, or pyramid and the hardness is calculated from the area or depth of indentation produced. Hegazy [26] demonstrated through experiments with four alloys, SS 304, nickel 200, zirconium-2.5% niobium, and Zircaloy-4, that the effective microhardness is significantly greater than the bulk hardness. As shown in Fig. 6, microhardness decreases with increasing depth of the indenter until bulk hardness is obtained. Hegazy concluded that this increase in the plastic yield stress (microhardness) of the metals near the free surface is a result of local extreme work hardening or some surface strengthening mechanism. He derived empirical correlations to account for the decrease in contact microhardness of the softer surface with increasing depth of penetration of asperities on the harder surface:

$$H_\nu = c_1(d'_\nu)^{c_2} \tag{9}$$

where H_ν is the Vickers microhardness in GPa, $d'_\nu = d_\nu/d_0$ and $d_0 = 1$ μm, d_ν is the Vickers indentation diagonal in μm, and c_1 and c_2 are correlation coefficients determined from Vickers microhardness measurements. Table 2 shows c_1 and c_2 for some materials. Relating the hardness of a microcontact to the mean size of microcontacts, Hegazy [26] suggested a correlation for effective microhardness,

$$H_{mic} = c_1\left(0.95\frac{\sigma'}{m}\right)^{c_2} \tag{10}$$

where $\sigma' = \sigma/\sigma_0$, $\sigma_0 = 1$ μm, and σ is the surface roughness in micrometers. Microhardness depends on several parameters: surface roughness, slope of asperities, method of surface preparation, and applied pressure. Song and Yovanovich [27] related H_{mic} to the surface parameters and nominal pressure

$$\frac{P}{H_{mic}} = \left(\frac{P}{c_1(1.62\sigma'/m)^{c_2}}\right)^{1/(1+0.071c_2)} \tag{11}$$

Sridhar and Yovanovich [28] suggested empirical relations to estimate Vickers microhardness coefficients, using the bulk hardness of the material. Two least-square-cubic fit expressions were reported,

$$c_1 = H_{BGM}(4.0 - 5.77\kappa + 4.0\kappa^2 - 0.61\kappa^3)$$
$$c_2 = -0.57 + 0.82\kappa - 0.41\kappa^2 + 0.06\kappa^3 \tag{12}$$

where $\kappa = H_B/H_{BGM}$, H_B is the Brinell hardness of the bulk material, and $H_{BGM} = 3.178$ GPa. The above correlations are valid for the range $1.3 \leqslant H_B \leqslant 7.6$ GPa, the rms percent difference between data and calculated values were reported: 5.3% and 20.8% for c_1 and c_2, respectively. Milanez et al. [29] studied the effect of microhardness coefficients on TCR by comparing the TCR's computed from the measured versus the estimated, from Eq. (12), microhardness coefficients. They concluded that despite the difference between the measured and estimated values of microhardness coefficients, the TCR's predicted by both methods are in good agreement.

Table 2 Vickers microhardness coefficients [26]

Material	c_1 (GPa)	c_2
Zr-4	5.677	−0.278
Zr-2.5 wt% Nb	5.884	−0.267
Ni 200	6.304	−0.264
SS 304	6.271	−0.229

Mechanical Analysis

As previously mentioned, the focus of this paper is on spherical rough contacts, and other nonconforming joints such as wavy rough contacts are not reviewed. The open literature contains very few analytical models for the spherical rough contacts. Spherical rough contact analysis includes two problems at different scales, (i) the bulk or macroscale compression and (ii) the asperities or microscale deformation.

Different approaches can be taken to analyze the deformation of asperities by assuming plastic [19], elastic [1], or elastoplastic [30,31] regimes at microcontacts. The fundamental assumptions, which are common in most of the models, can be summarized as (i) contacting surfaces are rough, with a Gaussian asperity distribution; (ii) behavior of a given microcontact is independent of its neighbors; (iii) interfacial force on any microcontact spot acts normally, no friction; and (iv) the deformation mechanics, i.e., the stress and displacement fields, are uniquely determined by the shape of the equivalent surface.

Abott and Firestone [32] developed the most widely used model for a fully plastic contact. Their model assumes that the asperities are flattened or equivalently penetrate into the smooth surface without any change in the shape of the noncontacting part of surfaces. Since the real area of contact is much smaller than the apparent contact area, the pressure at the asperities must be sufficiently large that it is comparable with the strength of the materials of the contacting bodies. Bowden and Tabor [33] and Holm [34] suggested that these contact pressures are equal to the flow pressure of the softer of the two contacting materials and the normal load is then supported by the plastic flow of its asperities. The real contact area is then proportional to the load, $A_r/A_a = P_m/H_{mic}$, where P_m is the mean apparent contact pressure. Cooper et al. [19] derived relationships for the real contact area, mean microcontact size, and number of microcontacts based on the level-crossing theory and using the sum surface approximation.

For applications in which the contacting surfaces meet many times, Archard [35] pointed out that the asperities may flow plastically at first, but they must reach a steady state in which the load is supported elastically. It has been observed through experiments that the real contact area is proportional to the load [2]. However, if elastic deformation is assumed for asperities, using the Hertzian theory, the real contact area will not be linearly proportional to the load, instead one obtains $A_r \propto F^{2/3}$. Archard [35] solved this problem by proposing that the surface asperities have microasperities

and microasperities have micro-microasperities, and so on. By adding several levels of asperities, Archard showed that $A_r \propto F$. Greenwood and Williamson (GW) [1] subsequently developed an elastic contact model; they proposed that as the load increases new microcontacts are nucleated while the mean size of microcontacts remains constant. The GW model also satisfied the observed proportionality $A_r \propto F$. As a result, an *effective elastic microhardness* can be defined for elastic models which shows that the assumption of elastic and/or plastic deformation of asperities leads to very similar results [1,36]. According to the GW model, the summits or "peaks" on a surface profile are the points higher than their immediate neighbors at the sampling interval used. Recently Greenwood and Wu [37] reviewed the assumptions of the GW model and concluded that "*the GW definition of peaks is wrong and gives a false idea of both number and the radius of curvature of asperities*." Greenwood and Wu proposed to return to the Archard idea that roughness consists of roughness on roughness and that the contact may be plastic at light loads but it becomes elastic at heavier loads. Based on the fractal characterization, Majumdar and Bhushan [38] developed a model for contact between two isotropic rough surfaces. According to their model, all contact spots of area less than a critical area are deformed plastically. This is due to the fact that smaller asperities have smaller radii of curvature and therefore are more likely to undergo plastic deformation. By increasing the load, these small plastic deformations join to form elastic contact spots.

The first in-depth analytical study to investigate the effect of roughness on elastic spherical bodies was performed by Greenwood and Tripp (GT) [36]. The microscale part of the GT model was based on the same assumptions as the GW model for microcontacts. Moreover, the bulk deformation was assumed to be elastic. Greenwood and Tripp [36] reported a complete set of relationships and solved it numerically. The most important trends in the GT model were that an increase in roughness resulted in a decrease in the pressure and an increase in the contact area. The GT model was a significant achievement, however its limitations are (i) the GT model was presented as a set of relationships; applying the model is complex and requires numerically intensive solutions. Also they did not propose a pressure distribution that accounts for roughness, and (ii) two of its input parameters, i.e., summits radius β and density η cannot be measured directly and must be estimated through statistical calculations. These parameters are sensitive to the surface measurements [21,27]. Mikic and Roca [39] developed an alternative numerical model by assuming plastic deformation of asperities and presented similar trends to those of the GT model. Mikic and Roca did not report relations to calculate the contact parameters. Greenwood et al. [40] introduced a nondimensional parameter α called the roughness parameter that governs primarily the rough spherical contact as

$$\alpha = \frac{\sigma\rho}{a_H^2} = \sigma\left(\frac{16\rho E'^2}{9F^2}\right)^{1/3} \tag{13}$$

Greenwood et al. [40] showed that the controlling nondimensional parameters in both [36] and [39] models can be written in terms of α. They concluded, for rough spherical contacts, that it is unimportant whether the asperities deform elastically or plastically; the contact pressure is predominantly governed by α. Further, if the value of α is less than 0.05, the effect of roughness is negligible and the Hertzian theory can be used.

Thermal Analysis

The complex nature of the TCR problem dictates making simplifying assumptions in order to develop thermophysical models. These complexities include the macro- and microscale thermal constriction/spreading resistances, the random distribution of size, shape, and location of microcontacts. Also the boundary condition of microcontacts, i.e., isothermal or isoflux, is not known. Therefore, in addition to the geometrical and mechanical assumptions, most existing thermal contact resistance models are based on the following common assumptions:

- contacting solids are isotropic, and thermal conductivity and physical parameters are constant
- contacting solids are thick relative to the roughness or waviness
- surfaces are clean and contact is static
- radiation heat transfer is negligible
- microcontacts are circular
- steady-state heat transfers at microcontacts
- microcontacts are isothermal; Cooper et al. [19] showed that all microcontacts must be at the same temperature, provided the conductivity in each body is independent of direction, position, and temperature
- microcontact spots are flat; it is justifiable by considering the fact that surface asperities usually have a very small slope [4].

Thermal contact models have been constructed based on the premise that within the macrocontact area a number of heat channels in the form of cylinders exist. The joint resistance under vacuum conditions can be calculated by superposition of microscopic and macroscopic resistances [3,4,22,23,41,14]:

$$R_j = R_{mic} + R_{mac} \tag{14}$$

The real shapes of microcontacts can be a wide variety of singly connected areas depending on the local profile of the contacting asperities. Yovanovich et al. [42] studied the steady-state thermal constriction resistance of a singly connected planar contact of arbitrary shape. By using an integral formulation and a semi-numerical integration process applicable to any shape, they proposed a definition for thermal constriction resistance based on the square root of the contact area. The square root of the contact area was found to be the characteristic dimension and a nondimensional constriction resistance based on the square root of area was proposed, which varied by less than 5% for all shapes considered. Therefore, the real shape of the microcontacts would be a second order effect and an equivalent circular contact, which has the same area, can represent the microcontacts.

Thermal Constriction/Spreading Resistance. The thermal spreading resistance is defined as the difference between the average temperature of the contact area and the average temperature of the heat sink, which is located far from the contact area, divided by the total heat flow rate Q [43,44]; $R = \Delta T/Q$. Thermal conductance is defined in the same manner as the film coefficient in convective heat transfer; $h = Q/(\Delta T A_a)$.

If it is assumed that the microcontacts are very small compared with the distance separating them from each other, the heat source on a half-space solution can be used [3]. Figure 7 illustrates the geometry of a circular heat source on a half-space. Classical steady-state solutions are available for the circular source areas of radius a on the surface of a half-space of thermal conductivity k, for two boundary conditions, isothermal and isoflux source. The spreading resistance for isothermal and isoflux boundary conditions are $R_{s,isothermal} = 1/(4ka)$ and $R_{s,isoflux} = 8/(3\pi^2 ka)$, respectively [5]. It can be seen that the difference between the spreading resistance for isoflux and isothermal sources is only 8%, $R_{s,isoflux} = 1.08 R_{s,isothermal}$.

As the microcontacts increase in number and grow in size, a constriction parameter, indicated by $\psi(\cdot)$, must be introduced to account for the interference between neighboring microcontacts. Roess [45] analytically determined the constriction parameter for the heat flow through a flux tube. Figure 8 illustrates the geometry of two flux tubes in a series. An equivalent long cylinder of radius, b, is associated with each microcontact of radius a. The total area of these flux tubes is equal to the interface apparent area. Consid-

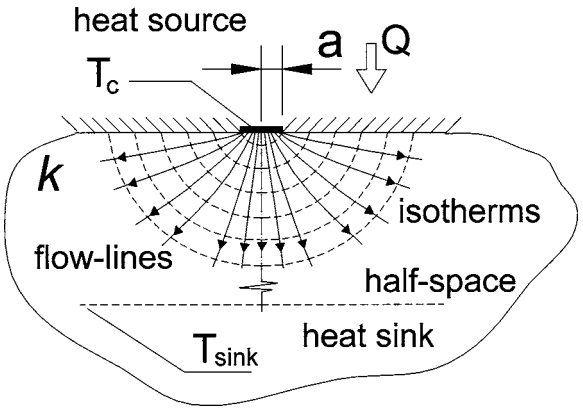

Fig. 7 Circular heat source on half-space

ering the geometrical symmetry, constriction and spreading resistance are identical and in series, $\psi_{spreading}=\psi_{constriction}=\psi$, Roess [45] suggested an expression in the form of

$$R_{two\ flux\ tubes}=\frac{\psi(\varepsilon)}{4k_1a}+\frac{\psi(\varepsilon)}{4k_2a}=\frac{\psi(\varepsilon)}{2k_sa} \tag{15}$$

where $k_s=2k_1k_2/(k_1+k_2)$ is the harmonic mean of the thermal conductivities and $\varepsilon=a/b$. To overcome the mixed boundary value problem, Roess replaced the temperature boundary condition by a heat flux distribution proportional to $[1-(r/a)^2]^{-1/2}$ over the source $0\leqslant r\leqslant a$ and adiabatic outside the source $a<r\leqslant b$. Roess presented his results in the form of a series. Mikic and Rohsenow [4], using a superposition method, derived an expression for the thermal contact resistance for half of an elemental heat channel (semi-infinite cylinder), with an isothermal boundary condition. They found another solution for the mixed boundary condition of the flux tube by using a procedure similar to Roess [45]. They also studied thermal contact resistance of the flux tube with a finite length. It was shown that the influence of the finite length of the elemental heat channel on the contact resistance was negligible for all values of $l\geqslant b$, where l is the length of the flux tube. Later this expression was simplified by Cooper et al. [19] (see Table 3). Yovanovich [43] generalized the solution to include the case of uniform heat flux and arbitrary heat flux over the microcontact. A number of correlations for isothermal spreading resistance for the flux tube are listed in Table 3. Figure 9 shows the comparison between these correlations. It is observed that at the limit when $\varepsilon\rightarrow 0$, the flux tube spreading resistance factor approaches one, which is the case of a heat source on a half-space. Also the results from all these various correlations for spreading resistance factor show very good agreement for the range $0\leqslant\varepsilon\leqslant 0.3$, which is typically the range of interest in thermal contact resistance applications.

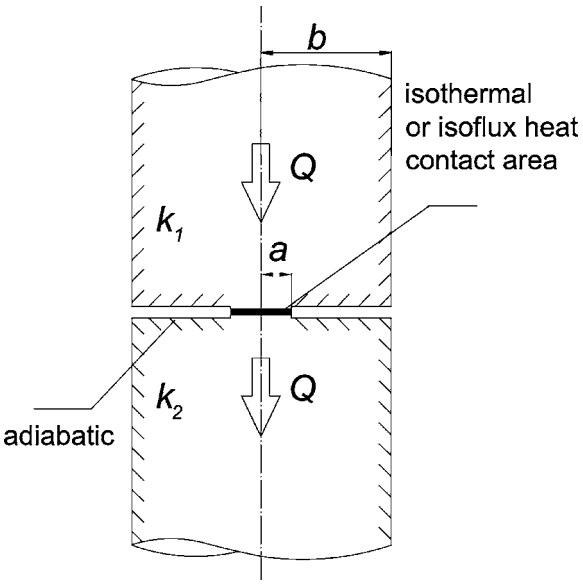

Fig. 8 Two flux tubes in series

Table 3 Thermal spreading resistance factor correlations, isothermal contact area

Reference	Correlation
Roess [45]	$1-1.4093\varepsilon+0.2959\varepsilon^3+0.0525\varepsilon^5+0.021\,041\varepsilon^7+0.0111\varepsilon^9+0.0063\varepsilon^{11}$
Mikic-Rohsenow [4]	$1-4\varepsilon/\pi$
Cooper et al. [19]	$(1-\varepsilon)^{1.5}$
Gibson [46]	$1-1.4092\varepsilon+0.3381\varepsilon^3+0.0679\varepsilon^5$
Negus-Yovanovich [47]	$1-1.4098\varepsilon+0.3441\varepsilon^3+0.0431\varepsilon^5+0.0227\varepsilon^7$

TCR Models for Conforming Rough Surfaces. During the last four decades, many experiments have been done and several correlations were proposed for nominally flat rough surfaces. Madhusudana and Fletcher [48] and Sridhar and Yovanovich [49] reviewed existing conforming rough models. Here only a few models will be reviewed, in particular those that are going to be compared with experimental data.

Cooper et al. [19] developed an analytical model, with the same assumptions that were discussed at the beginning of this section, for contact of flat rough surfaces in a vacuum:

$$R_c=\frac{4\sqrt{\pi}}{A_a\sqrt{2}k_s}\left(\frac{\sigma}{m}\right)\frac{\left[1-\sqrt{\frac{1}{2}\operatorname{erfc}(\lambda)}\right]^{1.5}}{\exp(-\lambda^2)} \tag{16}$$

where R_c, $\lambda=\operatorname{erfc}^{-1}(2P_m/H_{mic})$, and k_s are thermal contact resistance, dimensionless separation, and harmonic mean of thermal conductivities, respectively. Yovanovich [50] suggested a correlation based on the Cooper et al. [19] model, which is quite accurate for optically flat surfaces:

$$R_c=\frac{(\sigma/m)}{1.25A_ak_s(P/H_c)^{0.95}} \tag{17}$$

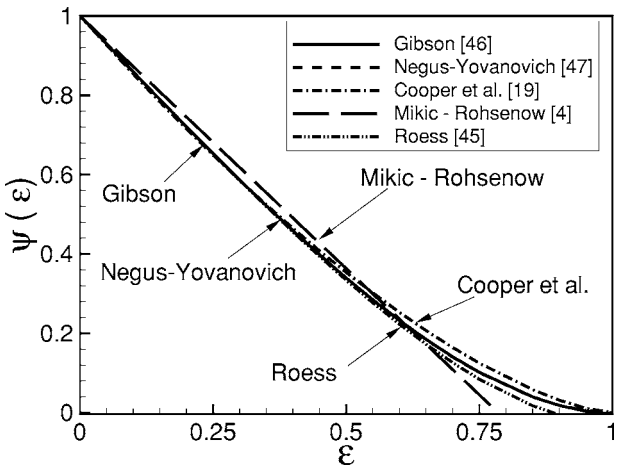

Fig. 9 Comparison between thermal spreading resistance correlations (Table 3) and isothermal contact area

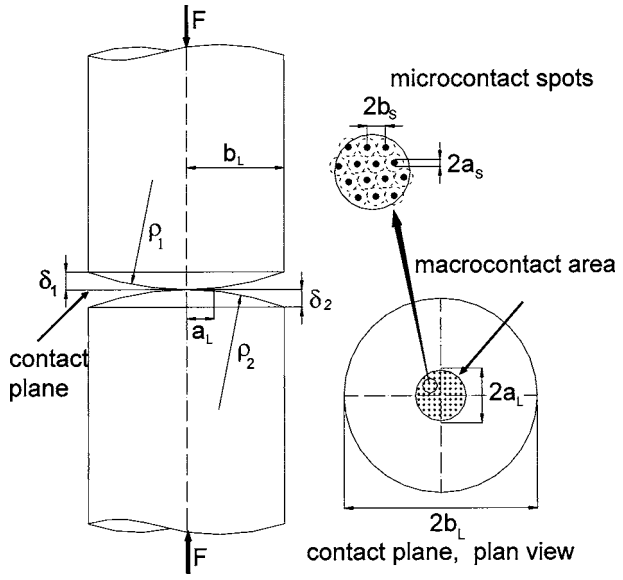

Fig. 10 Clausing and Chao [3] geometrical model

TCR Models for Nonconforming Rough Surfaces. Clausing and Chao [3] were the first to experimentally study the contact of rough nonflat surfaces. They also developed an analytical model, with the same assumptions that were discussed at the beginning of this section, for determining the thermal joint (macroscopic and microscopic) resistance for rough, spherical surfaces in contact under vacuum conditions. Their geometrical contact model is shown in Fig. 10; the effective radius of curvature of the contacting surfaces was found from Eq. (8). Using Roess [45] correlation (see Table 3), Clausing and Chao found the total microthermal resistance of identical, circular, isothermal microcontacts in the macrocontact area:

$$R_s = \frac{\psi(\varepsilon_s)}{2k_s a_s n_s} \tag{18}$$

The microscopic portion of the Clausing and Chao [6] model was based on the plastic deformation of asperities; a measured diamond pyramid hardness was used to consider the asperity hardness of the contacting surfaces. However, material microhardness was multiplied by ξ, an empirical correction factor introduced by Holm [34], to account for the effects of elastic deformation of asperities. The real contact area, A_r, then was calculated

$$A_r = \frac{F}{\xi H_{mic}} = n_s \pi a_s^2 \tag{19}$$

Additionally the following simplifications were made to enable an estimation of the microscopic constriction resistance:

- the microscopic contact spots were assumed to be identical and uniformly distributed, in a triangular array, over the macrocontact area (see Fig. 10)
- the average size of the microcontacts a_s was independent of load and it was of the same order of magnitude as the surface roughness, i.e., $a_s \equiv \sigma$.

They did not report the exact relationship between the microcontact radius and the roughness. In this study, it is assumed $a_s = \sigma$. They assumed an average value of $\xi = 0.3$ to take into account both plastic and elastic deformation of microcontacts. Also, a value of $\psi(\varepsilon_s) = 1$ was assumed, which means microcontacts were considered as isothermal circular heat sources on a half-space [6]; additionally they assumed $\xi\pi = 1$. With the above assumptions the microscopic thermal resistance became

$$R_s = \frac{\sigma H_{mic}}{2k_s F} \tag{20}$$

Neglecting the effect of roughness on the macrocontact area, Clausing and Chao determined the radius of the macrocontact area from the Hertzian theory, i.e., $a_L = a_H$. They reported a_L for elastic contact of spheres in the following form (assuming Poisson's ratio $\nu_1^2 = \nu_2^2 = 0.1$):

$$\varepsilon_L = \frac{a_H}{b_L} = 1.285\left[\left(\frac{P}{E_m}\right)\left(\frac{b_L}{\delta}\right)\right]^{1/3} \tag{21}$$

where $E_m = 2E_1E_2/(E_1 + E_2)$ and $\delta = \delta_1 + \delta_2$. Therefore, the thermal joint resistance, based on the Clausing and Chao [6] model, became

$$R_j = \frac{\sigma H_{mic}}{2k_s F} + \frac{\psi(\varepsilon_L)}{2k_s a_L} \tag{22}$$

where $\psi(\cdot)$ is the Roess [45] spreading factor (see Table 3). Clausing and Chao verified their model against experimental data and showed good agreement. Their model was suitable for situations in which the macroscopic constriction resistance was much greater than the microscopic resistance.

Kitscha [51] and Fisher [52] developed models similar to Clausing and Chao's [3] model and experimentally verified their models for relatively small radii of curvature and different levels of roughness. Burde [41] derived expressions for size distribution and number of microcontacts, which described the increase in the macroscopic contact radius for increasing roughness. His model showed good agreement with experimental data for spherical specimens with relatively small radii of curvature with different levels of roughness. Burde did not verify his model or perform experiments for surfaces approaching nominally flat. Also, results of his model were reported in the form of many plots, which are not convenient to use.

Mikic and Rohsenow [4] studied thermal contact resistance for various types of surface waviness and conditions, in particular; nominally flat rough surfaces in a vacuum, nominally flat rough surfaces in a fluid environment, smooth wavy surfaces in a vacuum environment (with one of the following three types of waviness involved: spherical, cylindrical in one direction, and cylindrical in two perpendicular directions), and rough spherical wavy surfaces in a vacuum. Thermal contact resistance for two spherical wavy rough surfaces was considered as the summation of a micro- and a macrothermal constriction resistance given by

$$R_j = \frac{\psi(a_{L,\text{eff}}/b_L)}{2k_s a_{L,\text{eff}}} + \frac{\psi(\varepsilon_s)}{2k_s a_s n_s} \tag{23}$$

where $\psi(\cdot)$ is the Mikic and Rohsenow [4] spreading factor (see Table 3). Similar to Clausing and Chao [3], the effective radius of curvature of the contacting surfaces was found from Eq. (8). The macrocontact area (for smooth surfaces) was determined by the Hertzian theory. Mikic and Rohsenow [4], assuming fully plastic deformation of asperities and equivalent surface approximation, derived expressions for the mean size and number of microcontacts that were used later by Cooper et al. [19]. Their model was based on the uniform distribution of identical microcontacts inside the macrocontact area. In the case of rough surface contacts, knowing that the macrocontact area would be larger than the one predicted by the Hertzian theory, they defined an effective macrocontact area. This area contained all the microcontact spots as if they had been uniformly distributed. Using this definition and the assumption that the mean surface would deform elastically, they suggested an iterative procedure for calculating the macrocontact radius. Mikic and Rohsenow verified their model against three experiments. Their computed ratios of macrocontact radius to Hertzian macrocontact radius were 1.6, 1.6, and 1.77 for each experiment and were considered constant throughout the tests, as

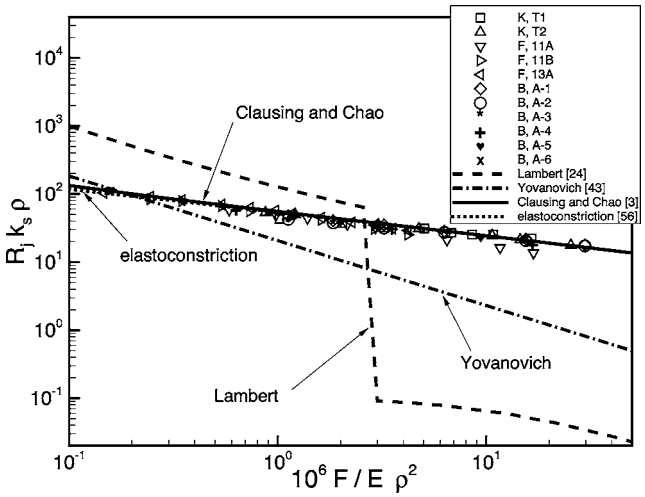

Fig. 11 Comparison with data at elasto-constriction limit

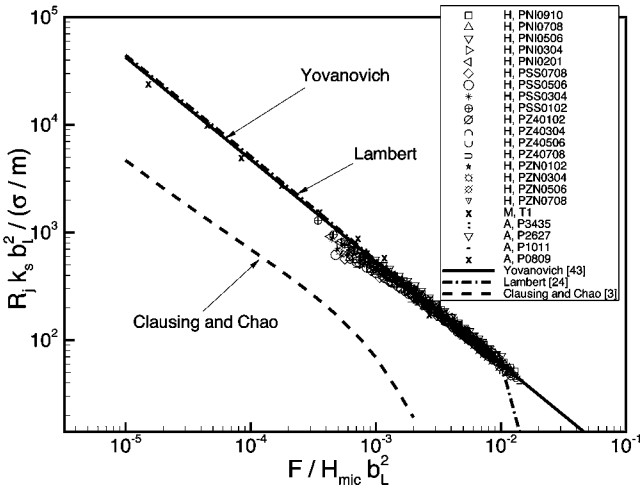

Fig. 12 Comparison with data at conforming rough limit

the external load increased. Mikic and Rohsenow did not derive the actual continuously varying pressure distribution for the contact of spherical rough surfaces. Additionally their expressions for effective macrocontact radius were very complex, and the iterative solution was quite tedious.

Later Mikic [53] derived expressions, based on the Mikic and Rohsenow [4] plastic model, for macroscopic and microscopic thermal resistances in a vacuum, which related thermal resistances (micro and macro) to arbitrary pressure distribution and surface properties. The derived relations were general in the sense that they did not require the knowledge of the effective macrocontact area and they could be applied for any symmetrical cylindrical or Cartesian pressure distribution at an interface. McMillan and Mikic [54] developed a numerical model and compared it with experimental data.

Lambert [24] studied the thermal contact resistance of two rough spheres in a vacuum. He started with the Greenwood and Tripp [36] elastic model for mechanical analysis, and the Mikic [53] thermal model as the basis for his thermal analysis. Lambert [24] was not able to solve the set of the mechanical relationships numerically and mentioned that "*the Greenwood and Tripp model is under-constrained, and convergence may be achieved for the physically impossible cases.*" To obtain numerical convergence, Lambert implemented results for the dimensionless axial minimum mean plane, reported by Tsukada and Anno [55], in the mechanical part of his model. The procedure for applying the Lambert [24] model (presented in appendix A of his thesis) was used to calculate thermal contact resistance in this study. He suggested two seventh-order polynomial expressions for pressure distribution and radius of macrocontact area as a function of dimensionless load. Lambert also introduced three dimensionless correction functions in the form of logarithmic polynomials in his thermal model, without specifying the origin and reasons for their presence. His approximate procedure was quite long and required computer-programming skills to apply. Also, logarithmic expressions for dimensionless macrocontact radius, a_L/a_H, showed a discontinuity, which caused a strange behavior in predicted thermal joint resistance (see Figs. 11 and 12). Lambert collected and summarized experimental data reported by many researchers and compared his model with experimental data. He showed a good agreement with experimental data.

Nishino et al. [23] studied the contact resistance of spherical rough surfaces in a vacuum under low applied load. Macroscopic and microscopic thermal contact resistance was calculated based on the Mikic [53] thermal model. Nishino et al. [23] used a pressure measuring colored film that provided information, by means of digital image processing, about the contact pressure distribution. They also verified their method experimentally with aluminum alloy specimens; the experimental data showed good agreement with their technique. They concluded that the macroscopic constriction resistance was predominant under the condition of low applied load. However, the Nishino et al. model required measurements with pressure sensitive film and they did not suggest a general relationship between contact pressure and surface profile and characteristics.

Comparison Between TCR Models and Data

The developed theoretical models by Clausing and Chao [3] [Eq. (22)], Yovanovich [50] [Eq. (17)], and Lambert [24] are compared with experimental data. References, material and physical properties, and surface characteristics of the experimental data are summarized in Table 4. As indicated in Table 4, the experimental data cover a relatively wide range of the experimental parameters.

The comparison is done at two extremes, conforming rough surfaces where the macro resistance is negligible and elastoconstriction limit where contacting surfaces have relatively small radii of curvature and the microresistance is almost negligible.

Thermal contact resistance for the above models was calculated for a base typical rough surface; the physical properties and surface characteristics are shown in Tables 5–7. Surface curvatures $\rho=14.3$ mm and $\rho=100$ m were chosen for elastoconstriction and conforming rough limits, respectively. Experimental data collected by Kitscha [51], Fisher [52], and Burde [41] were compared with the theoretical models in Fig. 11. The elastoconstriction approximation introduced by Yovanovich [56], which

Table 4 Parameter ranges for experimental data

Parameters
$57.3 \leq E' \leq 114.0$ GPa
$16.6 \leq k_s \leq 75.8$ W/mK
$0.12 \leq \sigma \leq 13.94$ μm
$0.04 \leq m \leq 0.34$
$0.013 \leq \rho \leq 120$ m

Table 5 Physical properties and surface characteristics of comparison base surface

$\sigma=1.3$ μm	$m=0.073$	$H_{mic}=3.92$ GPa
$b_L=7.15$ mm	$E'=114$ GPa	$k_s=40.7$ W/mK

Table 6 Summary of physical properties and surface characteristics, conforming rough limit

Reference	E'	σ	m	c_1	c_2	k_s	b_L
A,P3435	112.1	8.48	0.34	6.3	−0.26	67.1	14.3
A,P2627	112.1	1.23	0.14	6.3	−0.26	64.5	14.3
A,P1011	112.1	4.27	0.24	6.3	−0.26	67.7	14.3
A,P0809	112.1	4.29	0.24	6.3	−0.26	67.2	14.3
H,NI12	112.1	3.43	0.11	6.3	−0.26	75.3	12.5
H,NI34	112.1	4.24	0.19	6.3	−0.26	76.0	12.5
H,NI56	112.1	9.53	0.19	6.3	−0.26	75.9	12.5
H,NI78	112.1	13.9	0.23	6.3	−0.26	75.7	12.5
H,NI910	112.1	0.48	0.23	6.3	−0.26	75.8	12.5
H,SS12	112.1	2.71	0.07	6.3	−0.23	19.2	12.5
H,SS34	112.1	5.88	0.12	6.3	−0.23	19.1	12.5
H,SS56	112.1	10.9	0.15	6.3	−0.23	18.9	12.5
H,SS78	112.1	0.61	0.19	6.3	−0.23	18.9	12.5
H,Z412	57.3	2.75	0.05	3.3	−0.15	16.6	12.5
H,Z434	57.3	3.14	0.15	3.3	−0.15	17.5	12.5
H,Z456	57.3	7.92	0.13	3.3	−0.15	18.6	12.5
H,Z478	57.3	0.92	0.21	3.3	−0.15	18.6	12.5
H,ZN12	57.3	2.50	0.08	5.9	−0.27	21.3	12.5
H,ZN34	57.3	5.99	0.16	5.9	−0.27	21.2	12.5
H,ZN56	57.3	5.99	0.18	5.9	−0.27	21.2	12.5
H,ZN78	57.3	8.81	0.20	5.9	−0.27	21.2	12.5
M,SS1	113.8	0.72	0.04	6.3	−0.23	18.8	12.5

accounts only for macroresistance predicted by the Hertzian theory and neglects the microthermal resistance completely, was also included in the comparison. The elastoconstriction approximation was included to clearly demonstrate that the macroresistance is the dominating part of thermal joint resistance in the elastoconstriction limit, and the microthermal resistance is negligible. As can be seen in Fig. 11, the elastoconstriction approximation and the Clausing and Chao [3] model are very close and show good agreement with the data. The Lambert [24] model, as the result of its expression for macrocontact radius a_L, showed a strange behavior. As expected, the Yovanovich [56] model, which was developed for conforming rough surfaces, does not agree with the data.

Experimental data collected by Antonetti [57], Hegazy [26], and Milanez et al. [58] were compared with the theoretical models in Fig. 12. As shown, the Yovanovich [50] model showed good agreement with the data. Lambert [24] was very close to Yovanovich [50] in most of the comparison range, however the strange behavior in the predicted macrocontact area showed up as can be seen in the plot. The Clausing and Chao [3] model underpredicted thermal resistance in the conforming rough region.

Kitscha [55] and Fisher [56] did not report the surface slope, m; the Lambert [13] correlation was used to estimate these values (see Table 1). The exact values of radii of curvature for conforming rough surfaces were not reported. Since these surfaces were

Table 7 Summary of the physical properties and surface characteristics, elastoconstriction limit

Reference	E'	σ	m	ρ	c_1	c_2	k_s	b_L
B, A-1	114.0	0.63	0.04	0.0143	3.9	0	40.7	7.2
B, A-2	114.0	1.31	0.07	0.0143	3.9	0	40.7	7.2
B, A-3	114.0	2.44	0.22	0.0143	3.9	0	40.7	7.2
B, A-4	114.0	2.56	0.08	0.0191	4.4	0	40.7	7.2
B, A-5	114.0	2.59	0.10	0.0254	4.4	0	40.7	7.2
B, A-6	114.0	2.58	0.10	0.0381	4.4	0	40.7	7.2
F, 11A	113.1	0.12	⋯	0.0191	4.0	0	57.9	12.5
F, 11B	113.1	0.12	⋯	0.0381	4.0	0	57.9	12.5
F, 13A	113.1	0.06	⋯	0.0381	4.0	0	58.1	12.5
K, T1	113.8	0.76	⋯	0.0135	4.0	0	51.4	12.7
K, T2	113.8	0.13	⋯	0.0135	4.0	0	51.4	12.7

Table 8 Reseacher and specimen materials

Reference	Researcher	Specimen material(s)
A	Antonetti [57]	Ni 200
B	Burde [41]	SPS 245, Carbon Steel
F	Fisher [52]	Ni 200, Carbon Steel
H	Hegazy [26]	Ni 200 SS 304 Zircaloy4 Zr-2.5 % wt Nb
K	Kitscha [51]	Steel 1020, Carbon Steel
M	Milanez et al. [58]	SS 304

prepared to be optically flat, radii of curvature in the order of $\rho \approx 100(m)$ are considered for these surfaces. Table 8 indicates the researchers and the specimen materials used in the experiments.

Summary and Conclusion

Thermal contact resistance modeling and its components were studied. The modeling process was divided into three analyses: geometrical, mechanical, and thermal where each one included a macro- and microscale part.

Suggested empirical correlations to relate surface slopes, m, to surface roughness, σ, were summarized and compared with experimental data. The comparison showed that the uncertainty of the correlations was high; use of these correlations is not recommended unless only an estimation of m is required.

The common assumptions of the existing thermal analyses were summarized. Suggested correlations by different researchers for the flux tube spreading resistance were compared. It was observed that, at the limit, the correlations approached the heat source on a half-space solution. Also all the spreading resistance correlations showed good agreement for the applicable range.

Experimental data points obtained for five materials, namely SS 304, carbon steel, nickel 200, zirconium-2.5% niobium, and Zircaloy-4, were summarized and grouped into two limiting cases: conforming rough and elastoconstriction. These data were nondimensionalized and compared with TCR models at the two limiting cases. It was shown that none of the existing theoretical models covers both of the above-mentioned limiting cases.

This clearly shows the need to develop theoretical model(s) which can predict TCR over all cases including the above-mentioned limiting cases and the transition range where both roughness and out-of-flatness are present and their effects on contact resistance are of the same order.

Nomenclature

A = area, m^2
a = radius of contact, m
b = flux tube radius, m
c_1 = microhardness coefficients, Pa
c_2 = microhardness coefficients
d = mean plane separation, GW model units
d_v = Vickers indentation diagonal, μm
E = Young's modulus, Pa
E' = equivalent elastic modulus, Pa
F = external force, N
H, H_B = bulk hardness, Pa
H_{mic} = microhardness, Pa
H_{BGM} = geometric mean Brinell hardness, Pa
h = thermal contact conductance, $W/m^2 K$
k = thermal conductivity, W/mK
L = sampling length, m
m = effective mean absolute surface slope

m' = effective rms surface slope
n_s = number of microcontacts
P = pressure, Pa
Q = heat flow rate, W
q = heat flux, W/m^2
R = thermal contact resistance, K/W
R_a = arithmetic average surface roughness, m
R_q = rms surface roughness, m
r = radius, m
T = temperature, K
Y = mean surface plane separation, m

Greek

α = nondimensional parameter, $\equiv \sigma\rho/a_H^2$
δ = surface maximum out-of-flatness, m
ε = flux tube relative radius
κ = H_B/H_{BGM}
ν = Poisson's ratio
ψ = dimensionless spreading resistance
ρ = radius of curvature, m
σ = rms surface roughness, μm
ω = normal deformation, m
ξ = empirical correction factor

Subscripts

0 = value at origin
1, 2 = surface 1, 2
a = apparent
b = bulk
c = conduction, contact
eff = effective
g = gap
H = Hertz
j = joint
L = large (macro scale)
m = mean
mac = macro
mic = micro
r = real
s = small
ν = Vickers

References

[1] Greenwood, J. A., and Williamson, B. P., 1966, "Contact of Nominally Flat Surfaces," Proc. R. Soc. London, Ser. A, **295**, pp. 300–319.
[2] Tabor, D., 1951, *The Hardness of Metals*, Oxford University Press, Amen House, London.
[3] Clausing, A. M., and Chao, B. T., 1965, "Thermal Contact Resistance in a Vacuum Environment," Trans. ASME, Ser. C: J. Heat Transfer, **87**, pp. 243–251.
[4] Mikic, B. B., and Rohsenow, W. M., 1966, "Thermal Contact Conductance," Tech. Rep., Dept. of Mech. Eng. MIT, Cambridge, MA, NASA Contract No. NGR 22-009-065, September.
[5] Yovanovich, M. M., and Marotta, E. E., 2003, *Thermal Spreading and Contact Resistances*, Chap. 4, Heat Transfer Handbook, A. Bejan and D. Kraus (eds.), John Wiley and Sons, Inc., Hoboken.
[6] Clausing, A. M., and Chao, B. T., 1963, "Thermal Contact Resistance in a Vacuum Environment," Tech. Rep., University of Illinois, Urbana, IL, Report ME-TN-242-1, August.
[7] Bahrami, M., Yovanovich, M. M., and Culham, J. R., 2004, "Thermal Joint Resistances of Conforming Rough Contacts With Gas-Filled Gaps," AIAA J. Thermophys. Heat Transfer, **18**(3), pp. 1168–1174.
[8] Bahrami, M., Yovanovich, M. M., and Culham, J. R., 2004, "Thermal Joint Resistances of Conforming Rough Contacts With Gas-Filled Gaps," AIAA J. Thermophys. Heat Transfer, **18**(3), pp. 326–332.
[9] Liu, G., Wang, Q., and Ling, C., 1999, "A Survey of Current Models for Simulating Contact Between Rough Surfaces," Tribol. Trans., **42**(3), pp. 581–591.
[10] *Surface Texture: Surface Roughness, Waviness and Lay*, 1985, ANSI B46.1, American Society of Mechanical Engineers.
[11] Ling, F. F., 1958, "On Asperity Distributions of Metallic Surfaces," J. Appl. Phys., **29**(8), pp. 1168–1174.
[12] Tanner, L. H., and Fahoum, M., 1976, "A Study of the Surface Parameters of Ground and Lapped Metal Surfaces, Using Specular and Diffuse Reflection of Laser Light," Wear, **36**, pp. 299–316.
[13] Antonetti, V. W., White, T. D., and Simons, R. E., 1991, "An Approximate Thermal Contact Conductance Correlation," ASME 28th National Heat Transfer Conference, Minneapolis, MN, HTD-Vol. 170, pp. 35–42.
[14] Lambert, M. A., and Fletcher, L. S., 1997, "Thermal Contact Conductance of Spherical Rough Metals," ASME J. Heat Transfer, **119**(4), pp. 684–690.
[15] Francois, R. V., 2001, "Statistical Analysis of Asperities on a Rough Surface," Wear, **249**, pp. 401–408.
[16] Williamson, J. B., Pullen, J., and Hunt, R. T., 1969, "The Shape of Solid Surfaces," *Surface Mechanics*, ASME, New York, pp. 24–35.
[17] Greenwood, J. A., 1967, "The Area of Contact Between Rough Surfaces and Flats," J. Lubr. Technol., **89**, pp. 81–91.
[18] Bendat, J. S., 1958, *Principles and Applications of Random Noise Theory*, Wiley, New York.
[19] Cooper, M. G., Mikic, B. B., and Yovanovich, M. M., 1969, "Thermal Contact Conductance," Int. J. Heat Mass Transfer, **12**, pp. 279–300.
[20] Francis, H. A., 1976, "Application of Spherical Indentation Mechanics to Reversible and Irreversible Contact Between Rough Surfaces," Wear, **45**, pp. 221–269.
[21] Johnson, K. L., 1985, *Contact Mechanics*, Cambridge University Press, Cambridge, UK.
[22] Yovanovich, M. M., 1969, "Overall Constriction Resistance Between Contacting Rough, Wavy Surfaces," Int. J. Heat Mass Transfer, **12**, pp. 1517–1520.
[23] Nishino, K., Yamashita, S., and Torii, K., 1995, "Thermal Contact Conductance Under Low Applied Load in a Vacuum Environment," Exp. Therm. Fluid Sci., **10**, pp. 258–271.
[24] Lambert, M. A., 1995, "Thermal Contact Conductance of Spherical Rough Metals," Ph.D. thesis, Texas A & M University, Dept. of Mech. Eng., College Station, TX, USA.
[25] Mott, M. A., 1956, *Micro-Indentation Hardness Testing*, Butterworths Scientific Publications, London, UK.
[26] Hegazy, A. A., 1985, "Thermal Joint Conductance of Conforming Rough Surfaces: Effect of Surface Micro-Hardness Variation," Ph.D. thesis, University of Waterloo, Dept. of Mech. Eng., Waterloo, Canada.
[27] Song, S., and Yovanovich, M. M., 1988, "Relative Contact Pressure: Dependence on Surface Roughness and Vickers Microhardness," J. Thermophys. Heat Transfer, **2**(1), pp. 43–47.
[28] Sridhar, M. R., and Yovanovich, M., 1996, "Empirical Methods to Predict Vickers Microhardness," Wear, **193**, pp. 91–98.
[29] Milanez, F. H., Culham, J. R., and Yovanovich, M. M., 2003, "Comparisons Between Plastic Contact Hardness Models and Experiments," AIAA paper no. 2003-0160, 41th AIAA Aerospace Meeting and Exhibit, January 6–9, Reno, NV.
[30] Chang, W. R., Etison, I., and Bogy, D. B., 1987, "An Elastic-Plastic Model for the Contact of Rough Surfaces," ASME J. Tribol., **109**, pp. 257–253.
[31] Zhao, Y., Maietta, D. M., and Chang, L., 2000, "An Asperity Model Incorporating the Transition From Elastic Deformation to Fully Plastic Flow," ASME J. Tribol., **122**, pp. 86–93.
[32] Abott, E. J., and Firestone, F. A., 1933, "Specifying Surface Quality," Mech. Eng. (Am. Soc. Mech. Eng.), **55**, pp. 569–578.
[33] Bowden, F. P., and Tabor, D., 1951, *Friction and Lubrication of Solids*, Oxford University Press, London, UK.
[34] Holm, R., 1958, *Electrical Contacts 3rd Ed.*, Springer Verlag, Berlin.
[35] Archard, J. F., 1953, "Contact and Rubbing of Flat Surface," J. Appl. Phys., **24**, pp. 981–988.
[36] Greenwood, J. A., and Tripp, J. H., 1967, "The Elastic Contact of Rough Spheres," Trans. ASME, J. Appl. Mech., **89**(1), pp. 153–159.
[37] Greenwood, J. A., and Wu, J. J., 2001, "Surface Roughness and Contact: An Apology," Meccanica, **36**, pp. 617–630.
[38] Majumdar, A., and Bhushan, B., 1991, "Fractal Model of Elastic-Plastic Contact Between Rough Surfaces," ASME J. Tribol., **113**, pp. 1–11.
[39] Mikic, B. B., and Roca, R. T., 1974, "A Solution to the Contact of Two Rough Spherical Surfaces," ASME J. Appl. Mech., **96**, pp. 801–803.
[40] Greenwood, J. A., Johnson, K. L., and Matsubara, M., 1984, "A Surface Roughness Parameter in Hertz Contact," Wear, **100**, pp. 47–57.
[41] Burde, S. S., 1977, "Thermal Contact Resistance Between Smooth Spheres and Rough Flats," Ph.D. thesis, University of Waterloo, Dept. of Mech. Eng., Weterloo, Canada.
[42] Yovanovich, M. M., Burde, S. S., and Thompson, C. C., 1976, "Thermal Constriction Resistance of Arbitrary Planar Contacts With Constant Flux," AIAA Pap., paper no. 76-440, **56**, pp. 126–139.
[43] Yovanovich, M. M., 1976, "Thermal Constriction Resistance of Contacts on a Half-Space: Integral Formulation," in *AIAA Progress in Astronautics and Aeronautics, Radiative and Thermal Control, Vol. 49*, AIAA, New York, pp. 397–418.
[44] Carslaw, H. S., and Jaeger, J. C., 1959, *Conduction of Heat in Solids*, 2nd. Edition, Oxford University Press, London, UK.
[45] Roess, L. C., 1950, "Theory of Spreading Conductance," Beacon Laboratories of Texas, Beacon, NY, Appendix A (unpublished paper).
[46] Gibson, R. D., 1976, "The Contact Resistance of a Semi-Infinite Cylinder in a Vacuum," Appl. Energy, **2**, pp. 57–65.
[47] Negus, K. J., and Yovanovich, M. M., 1984, "Application of the Method of Optimized Images to the Steady Three Dimensional Conduction Problems," ASME, 84-WA/HT-110.
[48] Madhusudana, C. V., and Fletcher, L. S., 1981, "Thermal Contact Conductance: A Review of Recent Literature," Tech. Rep., Texas A & M University, College Station, TX, USA, September.
[49] Sridhar, M. R., and Yovanovich, M., 1993, "Critical Review of Elastic and

Plastic Thermal Conductance Models and Comparison With Experiment," paper no. 93-2776, 28th AIAA Thermophysics Conference, Orlando, FL, July 6–9.
[50] Yovanovich, M. M., 1982, "Thermal Contact Correlations," AIAA paper no. 81-1164; also *Progress in Aeronautics and Aerodynamics: Spacecraft Radiative Transfer and Temperature Control*, edited by T. E. Horton, Vol. 83, pp. 83–95.
[51] Kitscha, W., 1982, "Thermal Resistance of the Sphere-Flat Contact," Master's thesis, University of Waterloo, Dept. of Mech. Eng., Waterloo, Canada.
[52] Fisher, N. F., 1987, "Thermal Constriction Resistance of Sphere/Layered Flat Contacts: Theory and Experiment," Master's thesis, University of Waterloo, Dept. of Mech. Eng., Waterloo, Canada.
[53] Mikic, B. B., 1970, "Thermal Constriction Resistance Due to Non-Uniform Surface Conditions: Contact Resistance at Non-Uniform Interface Pressure," Int. J. Heat Mass Transfer, **13**, pp. 1497–1500.
[54] McMillan, R., and Mikic, B. B., 1970, "Thermal Contact Resistance With Non-Uniform Interface Pressures," Tech. Rep., Dept. of Mech. Eng. MIT, Cambridge, MA, NASA Contract No. NGR 22-009-(477), November.
[55] Tsukada, T., and Anno, Y., 1979, "On the Approach Between a Sphere and a Rough Surface (1st. Report-Analysis of Contact Radius and Interface Pressure)," J. Jpn. Soc. Precis. Eng., **45**(4), pp. 473–479 (in Japanese).
[56] Yovanovich, M. M., 1986, "Recent Developments In Thermal Contact, Gap and Joint Conductance Theories and Experiment," ASME, Keynote Paper Delivered at Eighth International Heat Transfer Conference, San Francisco, CA, August 17–22, pp. 35–45.
[57] Antonetti, V. W., 1983, "On the Use of Metallic Coatings to Enhance Thermal Conductance," Ph.D. thesis, University of Waterloo, Dept. of Mech. Eng., Waterloo, Canada.
[58] Milanez, F. H., Yovanovich, M. M., and Mantelli, M. B. H., 2003, "Thermal Contact Conductance at Low Contact Pressures," J. Thermophys. Heat Transfer, **18**, pp. 37–44.

Majid Bahrami *is a post-doctoral fellow at the Microelectronics Heat Transfer Laboratory MHTL, Department of Mechanical Engineering, University of Waterloo, Ontario, Canada. He received a B.Sc. degree in mechanical engineering from Sharif University of Technology, Tehran, Iran in 1992. He followed his graduate studies in Amir Kabir University of Technology, Tehran, Iran, and received an M.A.Sc. in 1995. He received a Ph.D. from the Department of Mechanical Engineering at the University of Waterloo. His doctoral research, "Modeling of Thermal Joint Resistance of Rough Sphere-Flat Contacts in a Vacuum," includes analytical, experimental, and numerical modeling of several macro- and micro-scale physical phenomena in heat transfer and contact mechanics with an emphasis on microelectronics cooling and thermal management. He has authored 20 refereed journal and conference scientific papers.*

M. Michael Yovanovich *is a Distinguished Professor Emiritus of Mechanical Engineering, University of Waterloo, Waterloo, ON, Canada, and is the Principal Scientific Advisor to the Microelectronics Heat Transfer Laboratory (MHTL). His research in the field of thermal modeling includes analysis of complex heat conduction problems, natural and forced convection heat transfer from complex geometries, and contact resistance theory and applications. He has published more than 300 journal and conference papers and numerous technical reports. He has been a consultant to several North American nuclear, aerospace, and microelectronics industries and national laboratories.*

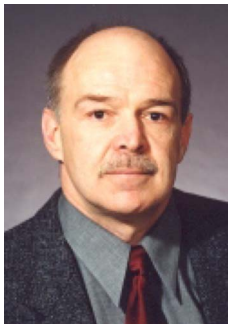

J. Richard Culham *is an Associate Professor of Mechanical Engineering at the University of Waterloo, Canada. He is the director and a founding member of the Microelectronics Heat Transfer Laboratory. Research interests include modeling and characterization of contacting interfaces and thermal interface materials, development of compact analytical and empirical models at micro- and nano-scales, natural and forced convection cooling, optimization of electronics systems using entropy generation minimization and the characterization of thermophysical properties in electronics and opto-electronics materials. Professor Culham has more than 100 publications in refereed journals and conferences in addition to numerous technical reports related to microelectronics cooling. He is a member of ASME, IEEE, and the Professional Engineers of Ontario.*

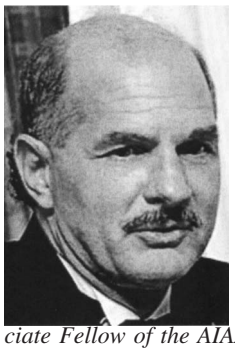

G. E. (Gerry) Schneider *was born in Waterloo, Ontario. He received a BASc (1973), MASc (1974), PhD (1977) in Mechanical Engineering from the University of Waterloo. Research includes heat conduction, heat pipes, and numerical methods in transport phenomena. Publications in refereed journals, 60+; refereed conference publications, 65+; invited publications and chapters for books, 13; books, 2; and many contract research reports. Session chair for 30+ technical sessions and Technical Program Chair for the AIAA 28th Thermphysics Conference. Associate Chair for Undergraduate Studies, Mechanical Engineering, 1984-1987; Associate Dean of Engineering, Undergraduate Studies, 1989–1998; currently Chair, Mechanical Engineering, University of Waterloo. As Associate Dean, oversaw the expansion of Engineering Exchange Programs from 7 to over 30. Program Review Committee Chair for an international program to establish a new technical university in Suranaree northeast of Bangkok. Board of Directors of the Computational Fluid Dynamics Society of Canada for nine years, and President for two years. Treasurer of the Society from 2002-2004. Member of the Editorial Advisory Board of Numerical Heat Transfer from its inception. Associate Fellow of the AIAA. Memeber of the AIAA Publications Committee, 1979-1986 and a member of the Operations Subcommittee. Associate Ediotr, Journal of Thermophysics and Heat Transfer, 1986-1993. Member of the AIAA Technical Committee for Thermophysics for over nine years; Chair of Committee, 1998-2000. Winner of the AIAA Sustained Service Award, 2003. Comerical, Multi-Engine, Instrument Flight Rules pilot license holder; Piper Seneca II twin-engine airplane owner. Professional Engineer in Ontario. Helped develop a new engineering program in Mechatronics Engineering a an expansion to my Department.*